


PAPER

# Online adaptive neural control of a robotic lower limb prosthesis

To cite this article: J A Spanias *et al* 2018 *J. Neural Eng.* **15** 016015

View the [article online](#) for updates and enhancements.

# Online adaptive neural control of a robotic lower limb prosthesis

J A Spanias<sup>1,2</sup> , A M Simon<sup>1,3</sup>, S B Finucane<sup>1</sup>, E J Perreault<sup>1,2,3</sup>  
and L J Hargrove<sup>1,2,3</sup>

<sup>1</sup> Center for Bionic Medicine, Shirley Ryan AbilityLab, 355 East Erie Street, Chicago, IL, United States of America

<sup>2</sup> Department of Biomedical Engineering, Northwestern University, Evanston, IL, United States of America

<sup>3</sup> Department of Physical Medicine and Rehabilitation, Northwestern University, Chicago, IL, United States of America

E-mail: [john.spanias@gmail.com](mailto:john.spanias@gmail.com)

Received 12 June 2017, revised 2 October 2017

Accepted for publication 11 October 2017


Published 9 January 2018



## Abstract

**Objective.** The purpose of this study was to develop and evaluate an adaptive intent recognition algorithm that continuously learns to incorporate a lower limb amputee's neural information (acquired via electromyography (EMG)) as they ambulate with a robotic leg prosthesis. **Approach.** We present a powered lower limb prosthesis that was configured to acquire the user's neural information and kinetic/kinematic information from embedded mechanical sensors, and identify and respond to the user's intent. We conducted an experiment with eight transfemoral amputees over multiple days. EMG and mechanical sensor data were collected while subjects using a powered knee/ankle prosthesis completed various ambulation activities such as walking on level ground, stairs, and ramps. Our adaptive intent recognition algorithm automatically transitioned the prosthesis into the different locomotion modes and continuously updated the user's model of neural data during ambulation. **Main results.** Our proposed algorithm accurately and consistently identified the user's intent over multiple days, despite changing neural signals. The algorithm incorporated 96.31% [0.91%] (mean, [standard error]) of neural information across multiple experimental sessions, and outperformed non-adaptive versions of our algorithm—with a 6.66% [3.16%] relative decrease in error rate. **Significance.** This study demonstrates that our adaptive intent recognition algorithm enables incorporation of neural information over long periods of use, allowing assistive robotic devices to accurately respond to the user's intent with low error rates.

**Keywords:** lower limb prostheses, electromyography, machine learning

 Supplementary material for this article is available [online](#)

(Some figures may appear in colour only in the online journal)

## 1. Introduction

Recent innovations in embedded computing, sensors, and batteries have enabled the development of powered exoskeletons [1] and prostheses [2] that could restore locomotion to individuals with disabilities. However, questions remain on how powered assistive robots should respond to user intent and operate in sync with users' remaining sensorimotor abilities.

These issues can only be partially addressed by interpreting the user's interaction with their environment through kinetic and kinematic sensors built into the device. Neural information extracted by processing electroencephalograms (EEG) [1, 3] or electromyograms (EMG) [4, 5] has been shown to be an excellent complement to data from inbuilt sensors; however, it is challenging to obtain and use such information reliably in a clinical environment. The goal of this study was to develop

a control system for a powered assistive device (specifically a powered knee-ankle prosthesis) that incorporates important neural information from EMG signals using a clinically viable methodology and that performs satisfactorily across multiple days. Achieving this goal would allow assistive robots to execute appropriate commands that are in accordance with the user's intent, addressing a major challenge in the clinical implementation of such devices.

Myoelectric interfaces have been used clinically to control robotic upper limb prostheses for decades, but have not yet been used to control lower limb prostheses—primarily because most commercially available devices are passive and do not require advanced control systems. Newly emerging robotic prosthetic legs can produce different mechanical responses depending on the mode of locomotion (e.g. walking on level ground, inclines, or stairs), and therefore require advanced control [6–10] (for an in-depth review of control strategies for powered assistive devices, see [11]). A current limitation in the control of robotic devices—the inability to automatically transition between these programmed modes of locomotion—could be addressed using a myoelectric interface [12, 13]. Specifically, EMG signals recorded from residual limb muscles can be inputted into a pattern recognition algorithm that can seamlessly transition the prosthesis between locomotion modes (a process we will refer to as *forward prediction*) [7, 9, 14–16]. Results have been promising: both offline and online studies have demonstrated that EMG signals significantly decrease the error rates of forward prediction algorithms when combined with the kinetic and kinematic information acquired from embedded mechanical sensors [4, 5, 17–19]. The obstacle that prevents full clinical implementation of this control approach is that these EMG-based algorithms are fixed and cannot track EMG signal changes that occur during daily prosthesis use (e.g. electrode shifts relative to the muscles of interest that occur during donning and doffing [20], loss of skin-electrode contact [21], or variations in electrode/skin impedance [22]). These changes cause the performance of the forward predictor, and thus the control system, to deteriorate. Clinical implementation requires an *adaptive* forward prediction algorithm that can track such changes and maintain the benefits of EMG over long-term use. The objective of this study was to develop and evaluate such an algorithm.

We previously demonstrated that classification errors caused by changes in EMG signals (due to electrode shift, etc) can be prevented by reverting to predictions based only on inbuilt mechanical sensor data when large EMG changes are detected [21], after which the algorithm must be retrained with updated EMG data. Because our algorithm used supervised learning, this required a method to automatically label new EMG data patterns with the user's intent. We previously accomplished this through *backwards estimation*, wherein we categorized the kinetic and kinematic gait profile after each stride of the prosthesis and labeled the new data pattern with the correct class label [23]. The advantage of using backwards estimation was the ability to correctly label patterns that the forward predictor misclassified (either because the prediction was difficult, or because signal changes caused errors, etc). Offline analyses have shown that these techniques are

an effective means of achieving adaptation [23]. In this study we completed an online analysis of the adaptive algorithm, in which individuals with transfemoral amputations walked on a robotic lower limb prosthesis.

In this online analysis, we must also consider changes to the control system for the robotic prosthesis, implemented since our previous studies on EMG-based pattern recognition, to improve control, ease of use, and pattern recognition performance. First, the robotic prosthesis used in the present study was equipped with additional mechanical sensors [2, 5], thus more sensor information was input into our forward prediction algorithm [24]. Second, various studies have investigated defining a critical timing window for mode transitions and found that delaying the timing of these transitions by a small window lowered the error rates of the forward prediction algorithm [25–27]. Thus we implemented this delay for the online experiments described in this study. Third, we implemented a mode-specific classifier architecture, which has been shown to improve classification accuracy in lower extremity applications [28]. As a result, the control system used in this study is very different from that used in our previous studies. Thus, we also investigated how these modifications affect performance of an online pattern recognition algorithm that is learning to reincorporate EMG into its predictions.

In this study, we present a fully integrated adaptive forward prediction system that can operate in real time during ambulation. We tested this system with eight individuals with transfemoral amputations. We demonstrate that our algorithm can (1) detect EMG signal changes, (2) automatically label new patterns of data, and (3) update algorithm parameters while the user is ambulating. To investigate adaptation to changes in EMG signals over time, we evaluated our algorithm using EMG data collected from subjects across multiple days, where we would expect changes in the quality of the EMG signals. We also conducted analyses that reveal the impact of control system modifications on the performance of the adaptive algorithm.

## 2. Methods

### 2.1. Experimental protocol

Eight subjects with a unilateral transfemoral amputation or knee disarticulation amputation completed the experiment (table 1), which was approved by the Northwestern University Institutional Review Board. Subjects' ages ranged from 24 to 67 years, heights between 1.63 and 1.93 m, and weights between 61.68 and 104.00 kg. Written and verbal consent was obtained from each subject involved.

Each subject was fitted with a socket that was custom-made at the Rehabilitation Institute of Chicago. The type of socket and method for collecting the surface EMG from the residual limbs of the subjects were selected based on the subject's definitive prosthesis. Three subjects wore a liner with embedded stainless steel electrodes (figure 1(A)). Two subjects used a skin-fit suction socket with embedded stainless steel electrodes (figure 1(B)). One subject used adhesive electrodes underneath a liner.

**Table 1.** Subject demographics.

Subject no.	Gender	Age (years)	Time post-amputation (years)	Weight (kg)	Etiology	Amputation level	Residual limb length (cm)
1	Male	59	48	83.9	Left traumatic	Transfemoral	22.5
2	Male	66	43	86.2	Right traumatic	Transfemoral	33.3
3	Male	31	21	86.2	Left sarcoma	Knee disarticulation	36.4
4	Female	47	28	61.7	Right traumatic	Transfemoral	23.7
5	Male	25	4	72.6	Right sarcoma	Transfemoral	29.3
6	Female	50	38	68.0	Right sarcoma	Transfemoral	21.1
7	Male	25	12	90.7	Right sarcoma	Transfemoral	38.0
8	Male	31	14	104.0	Left infection/sarcoma	Transfemoral	39.4
Mean [SD]	—	43.2 [16.5]	27.7 [16.4]	78.5 [11.0]	—	—	30.5 [7.4]

Eight channels of EMG data were acquired from each subject. Four pairs of electrodes were placed directly over the following muscles—rectus femoris (RF), tensor fasciae latae (TFL), semitendinosus (ST), and adductor magnus (AM). The other four channels were cross-pairings between the proximal (prox) and distal (dist) electrodes over the direct muscle sites ( $TFL_{prox} \times ST_{dist}$ ,  $ST_{prox} \times AM_{dist}$ ,  $AM_{prox} \times RF_{dist}$ , and  $RF_{prox} \times TFL_{dist}$ ). We recorded from these muscles because we identified them as among the most important muscles for lower limb movement classification in a previous study [29]. We were motivated to use cross-pairings between electrodes to acquire a measurement of the global activity of muscles within the residual limb. Similar grid-like configurations have been shown to be useful in upper-limb pattern classification applications [30]. The cross-pairings also provided four extra channels of EMG signals without having to localize any additional muscle sites. A certified prosthetist fitted and aligned a powered knee-ankle prosthesis, designed by the Center for Intelligent Mechatronics at Vanderbilt University (figure 2) [2]. Prior to the study, the powered prosthesis was configured for each subject for six different modes (standing, level-ground walking, stair ascent/descent, ramp ascent/descent) [7, 19, 31]. All subjects had previous experience using the powered prosthesis prior to completing the experimental protocol.

Subjects participated in two experimental sessions. The first session was conducted to collect data to train the adaptive forward predictor algorithm, while subjects were completing relevant mode transitions. Subjects used the powered prosthesis within a laboratory environment to complete ambulation activities including walking on level ground, walking up and down a 10° inclined surface, and stair ascent and descent on a 4-step staircase and a 3-step staircase (see supplementary materials video #1 ([stacks.iop.org/JNE/15/016015/mmedia](https://stacks.iop.org/JNE/15/016015/mmedia)) for a demonstration of the activities completed in this session). During this ‘offline session’, the experimenter used a key fob to transition the prosthesis between modes at critical points within the gait cycle [16]. Transitions between modes were programmed to occur 90 ms after a gait event (i.e. heel contact, toe-off, mid-swing, or mid-stance). All gait events were discrete points in time, and were determined using thresholds on mechanical sensor signals (e.g. load cell measurements, ankle dorsiflexion angle, shank inclination angle) and/or timers. Mechanical sensors thresholds were chosen so that mode transitions were triggered in a seamless way without

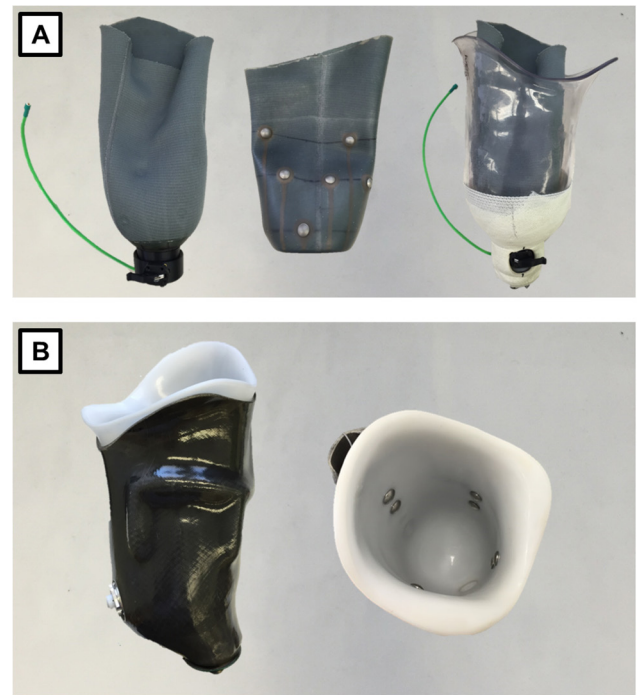


**Figure 1.** Experimental liners and sockets used to acquire EMG signals from the residual limb. Five subjects used a liner ((A), left) that went over the residual limb and had stainless steel electrodes embedded into the fabric ((A), middle). The subject then donned the rigid socket over the liner ((A), right), and connected to the electronics within the prosthesis. Two subjects wore just a rigid socket ((B), left) that had stainless steel electrodes embedded into the socket ((B), right).

any unnecessary or unnatural movement required by the user. More information about the definition of these gait events and how they were determined from the data can be found in our previous studies [27, 32, 33]. Collecting additional data after the gait event has been shown to improve pattern recognition performance in offline studies [25, 27], and transitioning between modes at this time point did not hinder the subjects’ ability to use the prosthesis.

The objective of the second experimental session was to determine whether the adaptive algorithm could automatically update the parameters of the EMG model (i.e. class means and covariances, explained below) used by the forward predictor during ambulation. For most subjects, this ‘online session’ occurred several weeks after the offline session; the subject



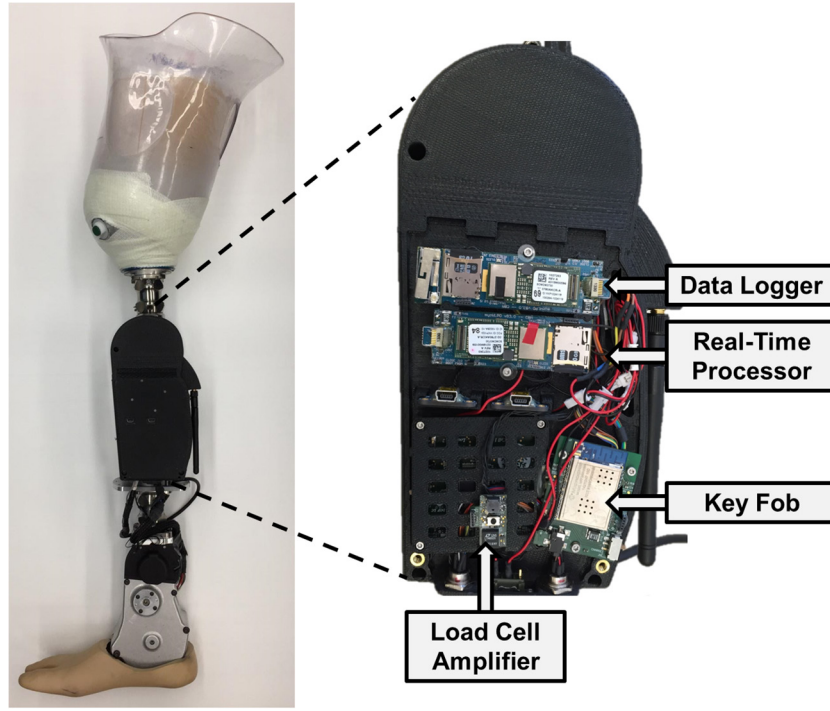


**Figure 2.** Powered prosthesis and embedded electronic hardware. Subjects ambulated with a powered knee-ankle prosthesis (left). The figure shows the socket attached to the prosthesis, the housing for the electronics, and the 6 DOF load used in the experiment. Various electronics were housed in the case, including a diagnostic data logger, a real-time processor, a wireless key fob receiver, and the load cell amplifier.

completed the same ambulation tasks with the prosthesis, but all mode transitions were controlled by the adaptive forward prediction algorithm, which was trained with the data collected in the first session.

## 2.2. Signal processing and control system architecture

Kinetic, kinematic, and inertial signals from 22 embedded mechanical sensors were recorded at 500 Hz. Mechanical sensor information included knee and ankle joint kinematics, motor currents, calculated thigh and shank inclination angles, and 6-degree of freedom (DOF) forces and moments. Eight channels of EMG were also recorded at 1000 Hz using a TI ADS 1299. These channels of information were used to complete the tasks of the adaptive algorithm: state machine control, forward prediction, backwards estimation, and adaptation. These tasks have been presented before separately using a hierarchical controller (figure 3), but had not previously been tested together in an online system. Here we present brief descriptions of each task:

**2.2.1. State machine control.** The joint torques of the prosthesis,  $\tau_i$ , were determined according to an impedance-based model used in multiple powered lower limb prosthetic applications (equation (1)) [2, 34]:

$$\tau_i = -k_i(\theta_i - \theta_{ei}) - b\dot{\theta}_i \quad (1)$$

where  $i$  denotes the knee or ankle joint,  $\theta$  is the joint angle, and  $\dot{\theta}$  is the joint angular velocity. A finite state machine [5, 19, 34, 35] modified the impedance parameters of the prosthesis,  $k$  (stiffness),  $\theta_d$  (equilibrium angle), and  $b$  (damping coefficient)

at different points in the gait cycle (i.e. the different states) and within different modes. The impedance parameters of each state were set according to previously defined control strategies [31]. Mechanical sensor data were used to transition the prosthesis between the different states of each mode. The selected torques were translated into motor command outputs that actuated the joint motors.

**2.2.2. Forward prediction.** During the online session, a forward prediction algorithm transitioned the prosthesis between the different modes. Forward prediction was accomplished by classifying EMG and mechanical sensor data patterns acquired *before the user's stride*, so that appropriate impedance parameters could be set for the prosthesis (figure 4(A)). The forward predictor was comprised of eight dynamic Bayesian network (DBN) [36] classifiers within a mode-specific classifier architecture [28]. Each classifier acted at a different part of the gait cycle (heel contact, mid-stance, toe off, and mid-swing) and within different modes. Information about the different classifiers, including when they were active, the number of output classes, and which modes they predicted can be found in [32, 33]. They were trained to predict six locomotion modes: standing, level-ground walking/ramp ascent, stair ascent/descent, and ramp descent. This architecture was chosen because it has been shown to improve pattern recognition performance in lower limb applications; detailed description of the control system can be found in [28]. Level-ground walking and ramp ascent were trained as a single class because the impedance parameter settings for these two modes were similar. For forward prediction, data were segmented into 300 ms windows. Since our control system used delayed mode

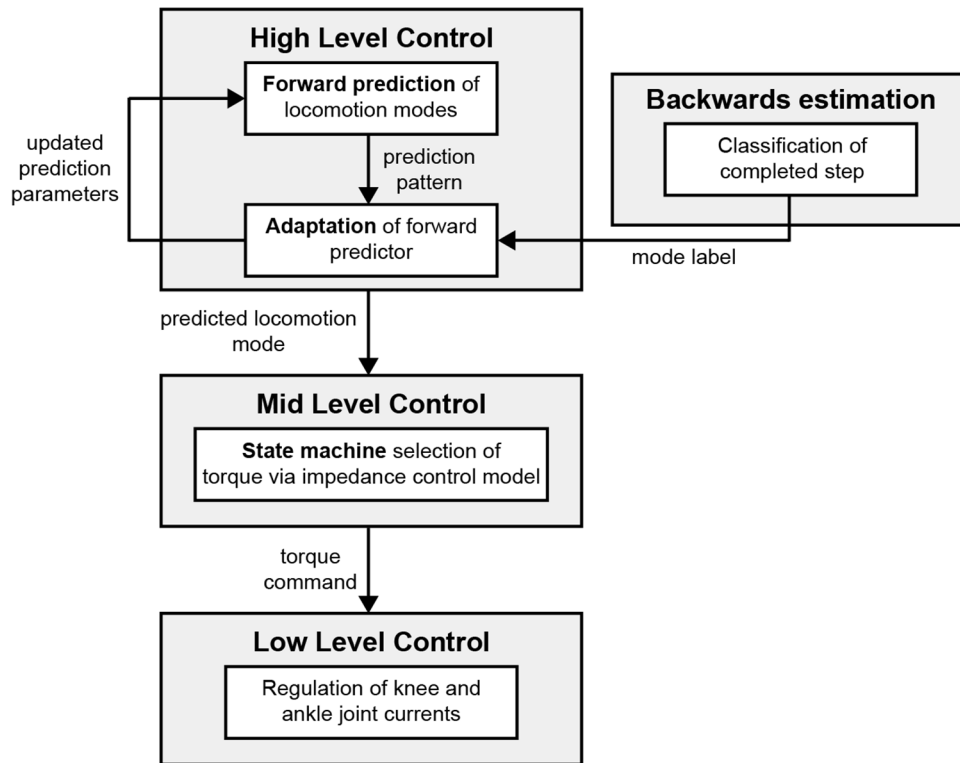


**Figure 3.** Block diagram of control system architecture. The tasks of the adaptive controller are first handled by a high level controller, which uses sensor data and forward prediction to determine the user's intent and select the desired locomotion mode. The high level controller also updates the forward predictor via adaptation, where new patterns are paired with class labels and used to update class means and covariances. The class label is provided by the backwards estimator, which classifies the user's completed step as one of the locomotion modes of the prosthesis. At the mid level, a state machine translates the predicted locomotion mode into the prosthesis' states of the gait cycle, and creates joint torque commands according to impedance control laws. The low level controller then takes these torque commands and translates them into appropriate joint motor currents.

transitions, the windows started 210ms before the gait event and ended 90ms after the gait event (figures 5(A) and (B)). The features extracted from the mechanical sensors included the mean, standard deviation, maximum, minimum, initial and final values of the window for each mechanical sensor channel [37]. Features extracted from the EMG channels included the mean absolute value, waveform length, zero crossing, slope sign changes [38], and the six autoregressive coefficients of a sixth-order autoregressive model extracted from each window for each EMG channel [39]. EMG and mechanical sensor feature sets were treated as statistically independent to facilitate adaptation of only EMG data, and to prevent overfitting. Pilot studies revealed that using all features from both sources of data resulted in overfitting. Thus, both EMG and mechanical sensor feature sets were reduced from 80 and 132 features, respectively, to 50 features using Principal Component Analysis [40]. The choice to reduce the total number of features down to 50 was found to achieve acceptable performance during pilot studies. Selecting the first 50 principal components explained over 99% of the variance in the data.

Each classifier within the forward predictor used a threshold based on the log-likelihood of the EMG feature vector to determine whether it was suitable to use EMG to make predictions [21]. New EMG patterns were compared to a model of all EMG patterns in a training dataset modeled as a Gaussian distribution (figures 5(C) and (D)). If the new EMG pattern had a log-likelihood that was more than three standard deviations

from the average log-likelihood of the feature vectors in the training set, then the new pattern was regarded as unsuitable for forward prediction. In this circumstance, the forward predictor only used mechanical sensor data to make predictions. Previous studies have shown that this technique was effective at preventing classification errors caused by disturbances in the EMG signals that occurred across experimental sessions [21]. We expected that our adaptive algorithm would initially disregard most of the novel EMG signals in the online session, but gradually reincorporate EMG into its predictions as the new model of EMG data was updated.

**2.2.3. Backwards estimation.** The backwards estimator acted *after the user completed a stride with the prosthesis* and provided a label for prediction patterns used for adaptation (figure 4(B)). The backward estimator used a linear discriminant analysis (LDA) classifier and classified the mechanical sensor data acquired from the entire stride. Thus, backwards estimation also differs from forward prediction in that it does not incorporate any prior knowledge of previous mode transitions (e.g. the time history information provided by DBNs [36] or the allowed mode transitions used by the mode-specific classifier architecture [28]). Mechanical sensor data were segmented into windows between consecutive heel contacts, such that the data window length was variable (figures 5(A) and (B)). Most windows were approximately 1.5 s and windows longer than 3 s were not classified (and

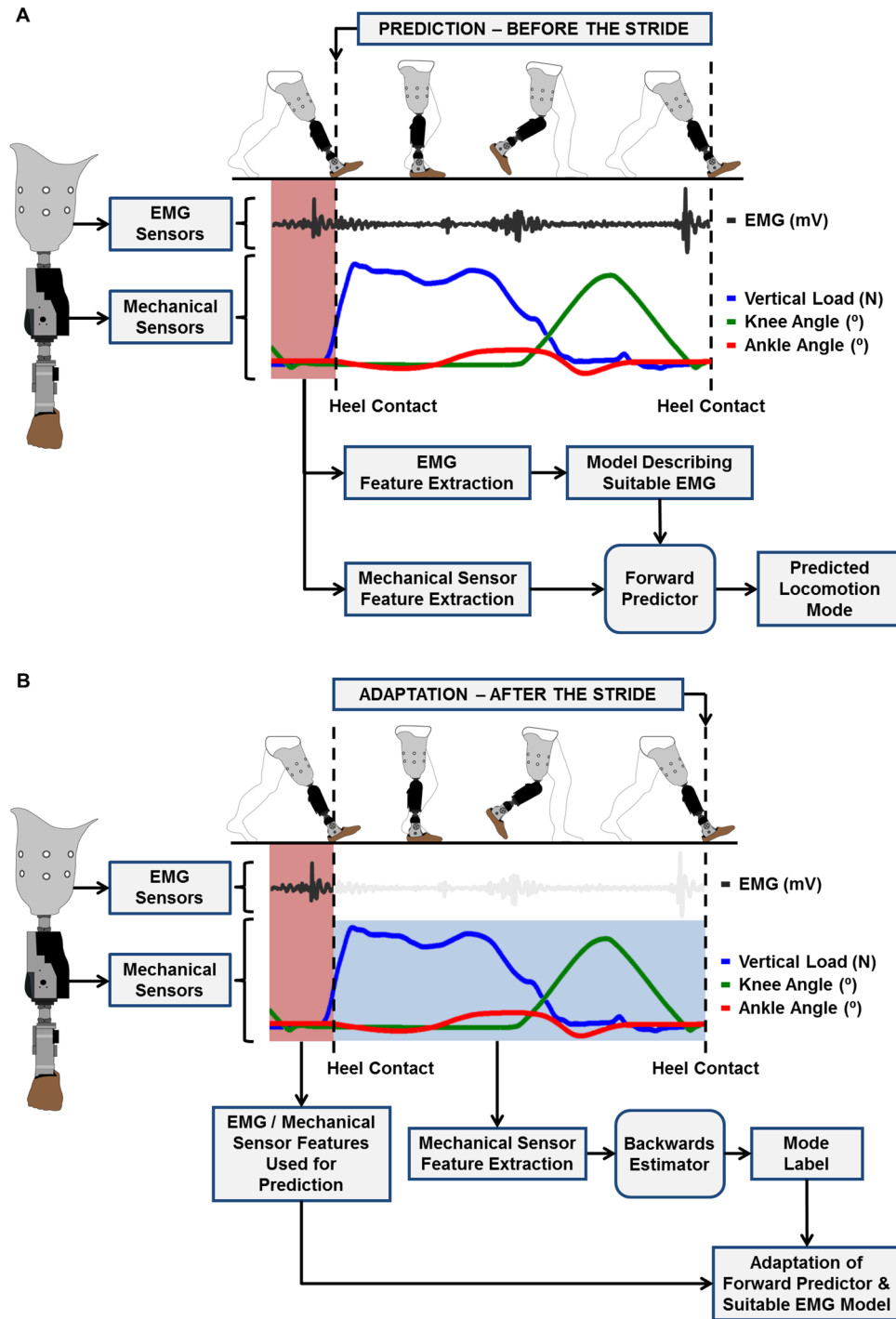


**Figure 4.** Overview of the adaptive algorithm. Components include forward prediction (A) and backwards estimation (B). In forward prediction, features are extracted from EMG data and mechanical sensor data acquired before the stride (red window) and classified by the forward predictor, which then transitions the prosthesis into the predicted mode. The forward predictor determines whether to use EMG in making its prediction by comparing the EMG feature vector to a model describing suitable EMG data. In backwards estimation, we wait until after the user completes their stride with the prosthesis and then classify the acquired mechanical sensor data (blue window) as one of the modes of the prosthesis. This provides a label for the pattern of data used for prediction, which is then used to adapt the parameters of the forward predictor and the model describing suitable EMG data.

consequently not used for adaptation). The same features as used for the forward predictor were extracted from these windows. The dimensionality of this feature set was reduced from 132 features down to 13 using uncorrelated linear discriminant analysis (ULDA) [41]. This method resulted in a dimensionally reduced combination of mechanical sensor

features. The backwards estimator classified the mechanical sensor data as one of the following classes: standing, level-ground walking, ramp descent, stair ascent/descent, and various classes where the user was ambulating in the incorrect mode (e.g. walking down a ramp in level-ground walking mode).

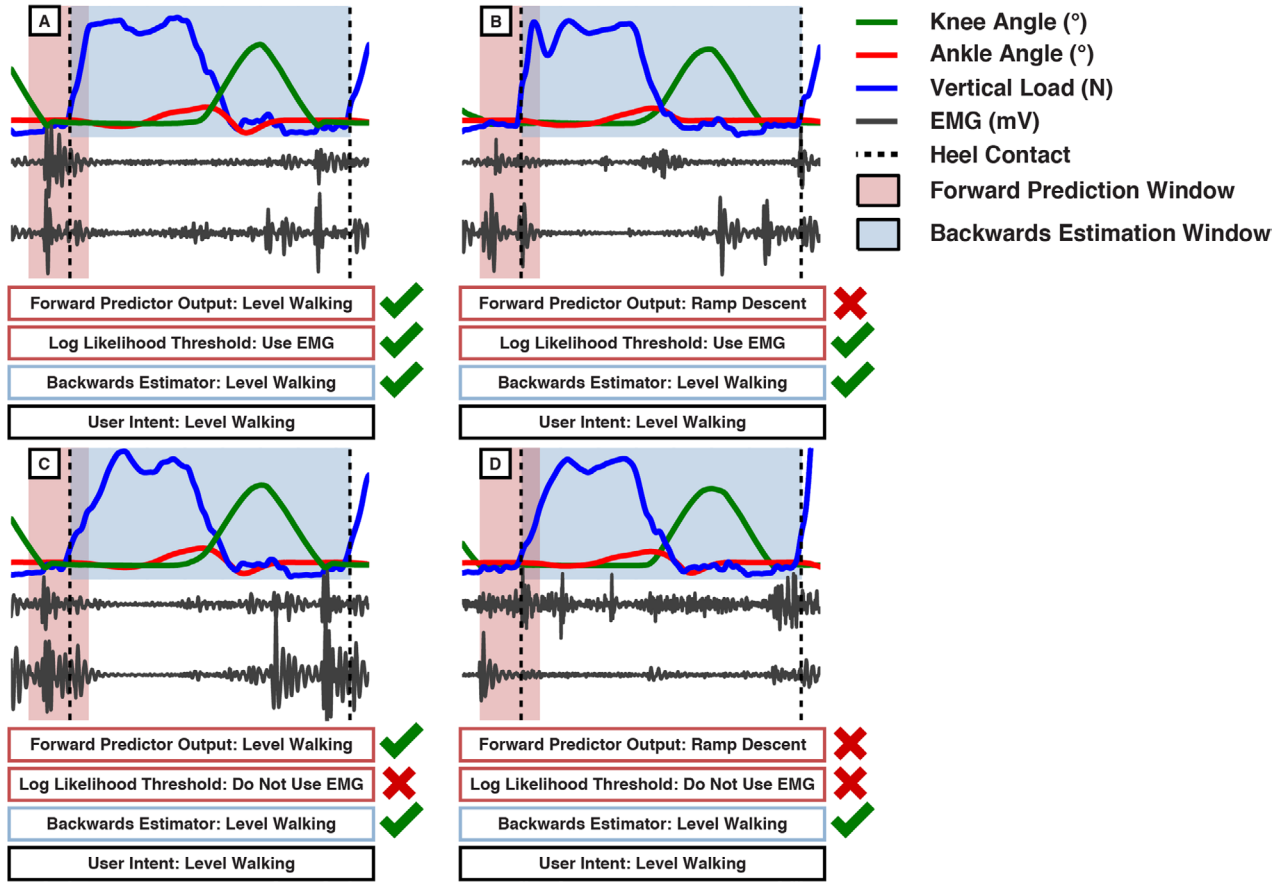


**Figure 5.** Illustrated examples of forward prediction, backwards estimation, and the log-likelihood threshold with real data acquired from a single representative subject. Forward prediction used a 300 ms window (the red shaded window) of data that began before a gait event (heel contact in this figure) and ended 90 ms after that gait event. If the log likelihood threshold, which used the same window as forward prediction, determined that it was appropriate to use EMG, then both EMG data and mechanical sensor data were used to make forward prediction (A) and (B); otherwise, only mechanical sensors were used (C) and (D). The backward estimator used the entire window of mechanical sensor data between heel contacts (the blue shaded window). This data was classified to provide a label for a pattern used to update the forward predictor. This figure shows an example where the output of both the forward predictor and the backwards estimator matched the true intent of the user (A) and (C), as well as a circumstance where the forward predictor was incorrect, but the backwards estimator still correctly labeled the data (B) and (D). Green checkmarks mean that the output of the forward predictor and/or the backwards estimator matched the user intent; the red cross means that the output of the forward predictor did not match the user intent. Similarly, a green checkmark means that EMG was used in the forward predictor's decision; a red cross means that EMG was not used.

**2.2.4. Adaptation of EMG.** After a pattern was labeled by the backwards estimator, it was used to adapt the EMG model of the forward predictor and the model describing the log likelihood threshold of EMG data. The parameters of these models were the class means,  $\mu_c$ , and covariances,  $\Sigma_c$ , of each classifier;  $c$  corresponds to the specific class. As the subject ambulated, the class means and covariances were updated with sequential estimation [42]. Equations (2) and (3) describe sequential estimation of a class mean,  $\mu_c$ , and class covariance,  $\Sigma_c$ , based on  $N$  observations and given the contribution of the newest pattern,  $x_N$ .

$$\mu_{c,N} = \mu_{c,N-1} + \frac{1}{N} (x_{c,N} - \mu_{c,N-1}) \quad (2)$$

$$\Sigma_{c,N} = \Sigma_{c,N-1} + \frac{1}{N} (x_N x_N^T - \Sigma_{c,N-1}) - \mu_{c,N} \mu_{c,N}^T. \quad (3)$$

These class means and covariances were then used to create updated classifiers. Class covariances were pooled ( $\Sigma$ ) and used with the updated means to calculate the new weights,

$W_c$ , and biases,  $w_c$ , of the classes of the DBN classifiers (equations (4) and (5)).

$$W_c = \sum^{-1} \mu_c \quad (4)$$

$$w_c = \frac{1}{2} \mu_c^T \sum^{-1} \mu_c. \quad (5)$$

Adaptation of EMG was completed on an embedded microcontroller (a Texas Instruments DM3730 processor running at 600 MHz) running a Linux operating system, to allow for execution of multithreaded processes. Specific tasks could be set to high or low priority depending on their computational intensity and real-time processing requirements. Tracking means and covariances was not computationally intensive; thus labeling each pattern and updating the class means and covariances was set to a high priority thread and completed after every heel contact. Updating the weights and biases of the classifiers was more computationally intensive because of the inversion of the pooled covariance matrix. Consequently,



this process was set to a low priority thread and was completed when additional processing time was available.

## 2.3. System evaluation

**2.3.1. Online analyses: performance of the online adaptive algorithm.** We observed how much EMG data was incorporated into forward predictor decisions throughout the online session. We also investigated whether the incorporation of EMG data would translate to a change in the error rate of the forward predictor. To evaluate the performance of the backwards estimator, we determined its error rate in the online session. We also investigated the algorithm's ability to run in real-time; we benchmarked the different components of the algorithm to determine the relative computational load of each task.

The patterns classified by the forward predictor and the backwards estimator were organized as steps (from heel contact to heel contact) completed with the prosthesis. Typically, a step contained a heel contact pattern and a toe-off pattern. A step was marked as an error if any of the patterns in that step were misclassified by the forward predictor. Similarly, if the forward predictor used EMG data with any of the patterns in a step, then the whole step was marked as having used EMG data.

We were interested in determining whether the amount of EMG data that the forward predictor used changed over the course of the online session (i.e. as the system was given more time to adapt). To track this variable over time, we first compiled all of the steps of the forward predictor and divided the total number of steps into quarters. Within each quarter, the percentage of steps where EMG was incorporated into the forward prediction was calculated. Thus, the amount of time the system spent adapting is described by the quarter of the experiment (where subsequent quarters mean more adaptation has occurred), and we could track changes in our chosen response variables over time by setting the quarter of the experiment as a factor in a statistical model. A one-way analysis of variance (ANOVA) was completed with quarter of the experiment as a factor, subject as a random factor, and the response was the percentage of patterns where EMG was used in a forward prediction. To evaluate whether the incorporation of EMG affected the performance of the forward predictor, we calculated the error rate of the forward predictor within every quarter. Error rates are reported as the pooled misclassification rates of the eight classifiers in the forward predictor. Also shown are steps taken within each mode for each quarter. ANOVA was completed with quarter of the experiment as a factor, subject as a random factor, and the response was the online error rate of the forward predictor. Post hoc tests were conducted on statistically significant variables of interest using Tukey's test. To further interpret the forward predictor's errors and their impact on the user, we also present confusion matrices. The confusion matrices show the different types of errors that occurred during the online session and which ones were most common (i.e. which classes caused the most confusion). This is useful because certain errors can cause large perturbations to the user, while others are unnoticeable [5].

To evaluate the automatic backwards estimation labeling strategy, we determined its online error rate. We chose this labeling strategy for its ability to outperform the strategy of using the output of the forward predictor as a label for new data [23]. A one-sided paired *t*-test was completed comparing the online error rate of the backwards estimator to the online error rate of the forward predictor.

We present the computational processing time for the real-time execution of the adaptive algorithm. We timed the following different components of our adaptive algorithm on our embedded system, a Texas Instruments DM3730 processor running at 600 MHz: baseline processing, feature extraction, forward prediction, backward estimation, and tracking of class means and covariances. Baseline processing represents the computation required for the prosthesis to function without the adaptive algorithm and includes data acquisition, state machine execution, and motor outputs. Based on our previous work, we required that our online system make forward predictions within a 30 ms frame increment [5]. We also calculated the average number of times classifiers were updated within a 10 min period.

## 2.3.2. Offline analyses.

**2.3.2.1. Comparison between adaptive system and non-adaptive systems.** We were interested in determining the benefit of including an adaptive mechanism as part of the EMG pattern recognition system. To accomplish this, we needed to determine how a non-adaptive system would have behaved during the online experimental session. Specifically, we were interested in how two non-adaptive systems—(1) a system that only used mechanical sensors and (2) a system that used the combination of mechanical sensors, EMG, and a log-likelihood threshold—would have behaved during an online session. In this offline analysis, we calculated how the forward predictors of these two systems performed when evaluated with data from online experimental sessions, and compared this performance with that of the online adaptive system. This comparison between adaptive and non-adaptive systems revealed the benefit of including an adaptive mechanism, and, more specifically, the benefit of updating the user's model of EMG data. ANOVA was completed with type of system as a factor, subject as a random factor, and error rate as the response. Post hoc tests were conducted on statistically significant variables of interest using Tukey's test.

**2.3.2.2. Benefit of EMG with the current control system.** To determine the impact of the control system modifications on algorithm performance, we compared the performance of our modified algorithm to that of an algorithm configured as in our previous studies. This previous configuration (which we will term the *null* configuration) was used with a previous generation of the prosthesis with fewer mechanical sensors, did not incorporate a 90 ms delay in its mode transitions (i.e. was a 'non-delayed system'), and used a different classifier architecture. This null configuration was simulated with our current dataset in an offline analysis, using combined data from the offline and online experimental sessions.

To simulate results with fewer mechanical sensors, we removed the inputs from mechanical sensor channels that were not available in the previous generation of the prosthesis. These included five degrees of freedom from the load cell and the calculated thigh and shank angles. Because all data were collected with a 90 ms delay for mode transitions, a non-delayed system could be simulated: data were segmented into 300 ms windows immediately preceding gait events (e.g. from 300 ms before heel contact to heel contact). Lastly, in our earlier control system each mode did not have its own classifier. Instead, all transitions were handled by a single classifier regardless of which mode the prosthesis was in, and we assumed that EMG features and mechanical sensor features were not independent (as in previous studies). This single pattern recognition architecture was used in this analysis.

We calculated forward prediction performance of the null configuration, without any system modifications, and then added each modification (expanded mechanical sensors, delayed mode transitions, and the mode specific classifier architecture) separately to determine the individual effect of each modification. We also calculated forward prediction performance with all combinations of control system modifications, including all modifications. For each condition, we calculated the performance of a forward predictor that only used mechanical sensor data and one that used a combination of mechanical sensor and EMG data. Performance is reported in terms of forward prediction error rate. Error rate was further separated into steady-state and transitional errors. Steady-state errors are those that occur when the prosthesis remains in one mode; transitional errors are those that occur when the prosthesis is switching between modes. We made the distinction between these two types of errors for this analysis because previous studies (which used a control system similar to the null configuration) also differentiated between these two types of errors, and thus it was beneficial in understanding the differences between the older and newer control systems. A repeated measures ANOVA was performed for both steady-state and transitional error with classification error as the response and type of control system (Null versus with all modifications) and type of forward predictor (mechanical sensors versus mechanical sensors and EMG) as fixed within-subject variables with interaction terms.

### 3. Results

All subjects were able to transition between the required locomotion modes and complete the different activities using the online system (see supplementary materials video #2 for a demonstration of a subject ambulating with the online system). The percentage of forward predictions where EMG was incorporated per quarter is shown in figure 6. In the first quarter of the online session, EMG was used in 68.86% [8.93%], mean (standard error) of forward predictions. The percentage of patterns where EMG was used increased in every following quarter, and by the end of the experiment the algorithm used EMG in 96.31% [0.91%] of forward predictions. The

percentage of EMG used in the first quarter was statistically different from that in the following quarter ( $p < 0.001$ ).

The overall error rate of the adaptive forward predictor was 4.03% [0.69%]. This level of performance was consistent across the experiment, with no statistical differences found between the online error rates in each quarter ( $p = 0.51$ ) (figure 6).

The offline error rate of the non-adaptive system that used only mechanical sensors was 4.44% [0.83%], and of the non-adaptive system that used the combination of mechanical sensors, EMG, and a log-likelihood threshold was 4.38% [0.80%] (figure 7). The difference in error rates between these two non-adaptive systems was not significant ( $p = 0.099$ ). The online error rate of the adaptive system was found to be significantly different from that of both non-adaptive systems ( $p = 0.013$  and  $p = 0.031$ , respectively).

The confusion matrices of the forward predictor in the online session averaged across subjects are in table 2. The table shows what types of errors the forward predictor made, where the percentage in a particular cell ( $i, j$ ) is the percentage of steps predicted to be in row  $i$  but known to be in column  $j$ . The class abbreviations are: ST = standing, LW = level walking, SA = stair ascent, RD = ramp descent, SD = stair descent. Steps that were supposed to be predicted as ramp descent were the most difficult for the forward predictor, and were mostly frequently classified as level walking (8.45% [3.50%]). Although these were the most common error, these misclassifications presented only a minor perturbation to the user. Because most patients could not ‘walk through’ this misclassification, these errors typically required the user to reattempt the transition onto the ramp, but did not endanger the user. Inappropriate transitions to ramp descent or stair descent during level walking are noteworthy because the user is not expecting a mode transition during steady-state walking. These errors occurred during 1.44% [0.51%] and 0.43% [0.15%] of level walking steps, respectively. Typically, the user could walk through these errors, and despite being unexpected and noticeable they did not usually disrupt ambulation. Other types of perturbations that were more severe (e.g. inappropriately transitioning to stair ascent while on level ground, or misclassifying a stair descent step as level walking) were more rare (0.23% [0.07%] and 0.96% [0.54%], respectively), but usually required the patient to take action to prevent a stumble or fall (e.g. use their hands to steady themselves with a rail or a wall, and/or reattempt the transition; see supplementary materials video #3 for a demonstration of an inappropriate transition into stair ascent). Similarly, the prosthesis rarely incorrectly transitioned to a different mode when the user was standing in place.

The backward estimator was able to label patterns used for adaptation with a low error rate of 1.64% [0.25%] (figure 8), which was significantly lower than the online error rate of the forward predictor, 4.03% [0.69%] ( $p = 0.024$ ).

The online computational time for the control system processes can be found in table 3. Baseline processing, backwards estimation, and feature extraction were the most time-intensive processes. The average time to execute all the relevant processes of the prosthesis while running the adaptive

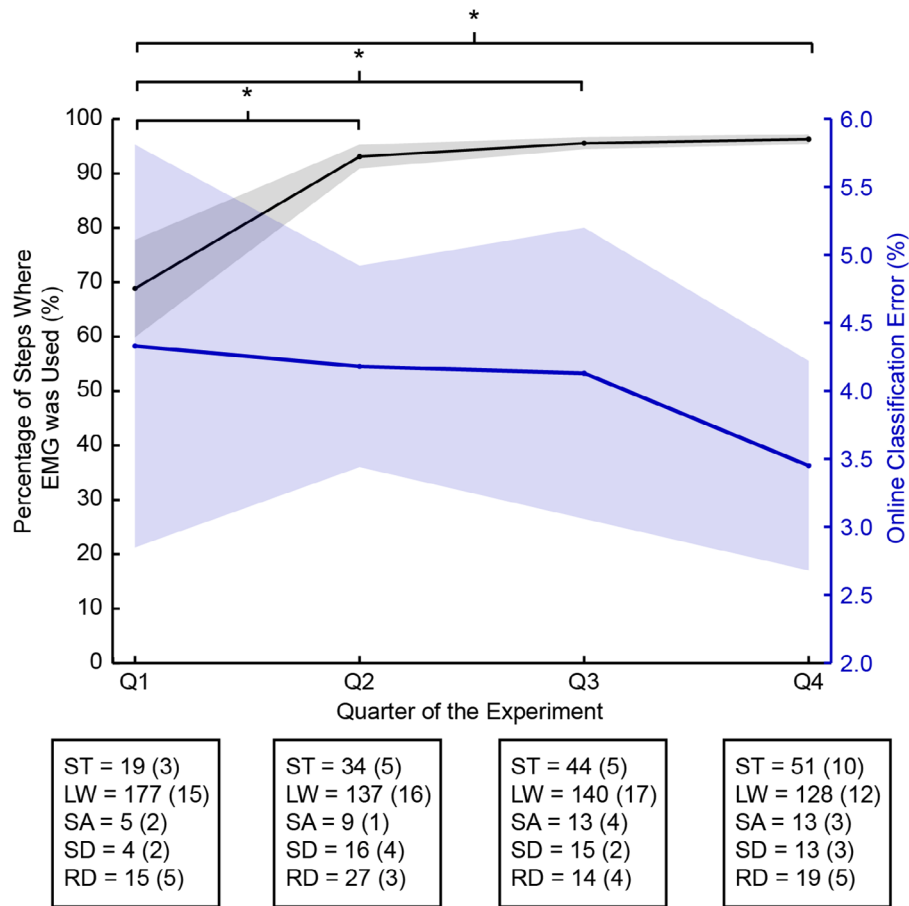


**Figure 6.** Online performance of adaptive forward predictor and percent of patterns where EMG was incorporated into the prediction throughout the experiment. All patterns classified by the adaptive forward predictor were divided into quarters (Q1–Q4). The figure shows the online error rate of the predictor (blue line) and the progression of EMG use throughout the experiment (black line). For each pattern, the pattern recognition algorithm used the combination of EMG data and mechanical sensor data, or only mechanical sensor data. To illustrate the activities completed, the true class of the patterns in each quarter is shown (ST = standing, LW = level walking, SA = stair ascent, SD = stair descent, RD = ramp descent). Data are averages of eight subjects ( $\pm 1$  SEM). \* denotes statistically significant differences ( $p < 0.05$ ).

algorithm was 22.9 ms [2.5 ms], well below our 30 ms requirement. As mentioned before, the process of tracking class means and covariances was set to a low priority thread and was completed when additional processing time was available. As a result, classifiers were updated periodically and less frequently than once per step. Within a 10 min period, the forward predictors were updated 125 times.

Performance was compared between forward predictors with no modifications (i.e. the null condition), with each individual modification, and all combinations of modifications (figure 9). When using the null control system, the forward predictor that used both mechanical sensor signals and EMG signals had lower error rates than the forward predictor that only used mechanical sensors (a 0.44% decrease for steady-state error; a 1.55% decrease for transitional error). Adding modifications to the control system typically reduced the error rates of both types of forward predictors. The lowest error rates were obtained when applying all modifications. When all modifications were added, the forward predictor that used both mechanical sensor and EMG data had higher error rates than the forward predictor that only used mechanical sensor data (a 0.01% increase for steady-state error; a 0.10% increase

for transitional error). The results of the ANOVA revealed that there was a significant effect due to the type of control system (null versus with all modifications) for both steady-state error ( $p < 0.001$ ) and transitional error ( $p < 0.001$ ). All other factors were found to be non-significant ( $p > 0.05$ ).

#### 4. Discussion

The goals of this study were to develop an adaptive intent recognition control algorithm for a robotic lower limb prosthesis that can utilize important neural information (EMG) and maintain control accuracy over multiple days—and to evaluate its performance in individuals with transfemoral amputations during online experiments. The resulting control system could respond to the user's intent in a variety of environments and across long periods of time.

The adaptive algorithm could appropriately select when to incorporate EMG into its forward predictions. Because EMG signals were likely different across experimental sessions as a result of donning and doffing the prosthesis, it was desirable that the algorithm did not initially incorporate all EMG into its forward predictions. In previous offline studies,

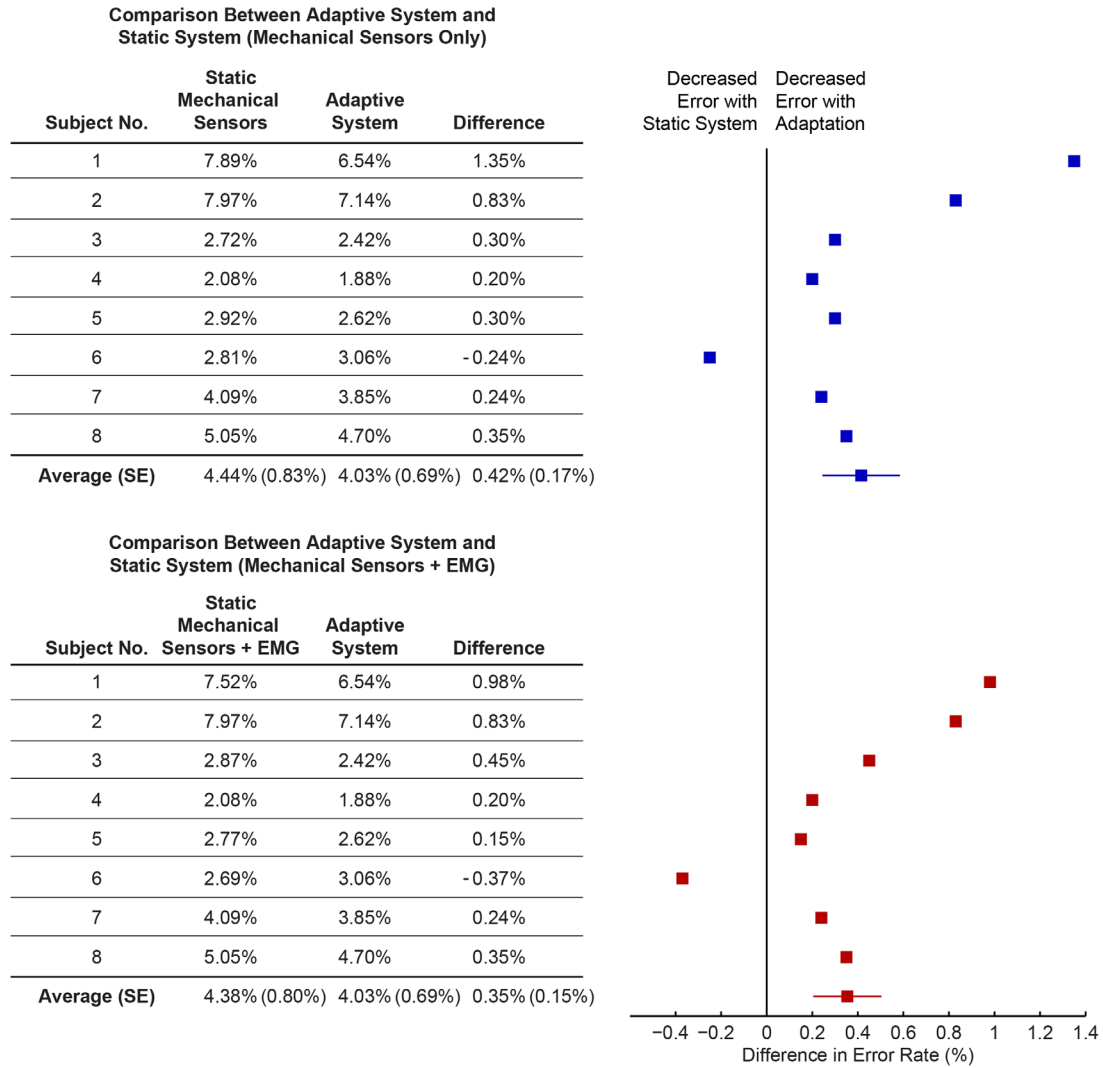


**Figure 7.** Performance differences between the online adaptive system and offline non-adaptive (static) systems. Performance (error rates) of the online adaptive system was compared to two different non-adaptive systems that—(1) only used mechanical sensors (top, blue) or (2) used a combination of mechanical sensors, EMG, and a log-likelihood threshold (bottom, red). The performance of the non-adaptive systems was determined by calculating how the forward predictors of these two systems performed when evaluated with data from online experimental session. The results for each subject and the average for all subjects are shown for each comparison in tables on the left. The difference in performance is shown graphically on the right. Data are averages of eight subjects ( $\pm 1$  SEM).

**Table 2.** Confusion matrix of online performance (%).

	ST	LW	SA	RD	SD
ST	99.63 [0.15]	0.00 [0.00]	0.44 [0.22]	2.20 [1.49]	0.51 [0.44]
LW	0.12 [0.12]	97.90 [0.63]	1.79 [0.59]	8.45 [3.50]	0.96 [0.54]
SA	0.10 [0.07]	0.23 [0.07]	97.42 [0.88]	0.00 [0.00]	0.28 [0.28]
RD	0.00 [0.00]	1.44 [0.51]	0.22 [0.22]	88.46 [4.57]	0.30 [0.30]
SD	0.14 [0.09]	0.43 [0.15]	0.12 [0.12]	0.88 [0.64]	97.94 [0.80]

we demonstrated that a log likelihood threshold can be used to determine whether to use both EMG and mechanical sensor signals to make a forward prediction, or to simply use mechanical sensors [21]. With this study, we verified that our proposed threshold performed as expected in real-time. This likely prevented forward prediction errors that would have occurred when using EMG data that contained disturbances or varied across days; reverting to using only mechanical sensors was a safer alternative.

We also show that the adaptive algorithm learned to reincorporate EMG over time. As subjects ambulated, our algorithm gathered new patterns of EMG data, labeled them with the user's intent, and updated the model of EMG training data. As a result, the model began to describe EMG data acquired from multiple experimental sessions, and the log-likelihood threshold, which was also updated in the process, allowed more EMG data to be used in forward predictions. Thus the percentage of EMG data incorporated into the forward



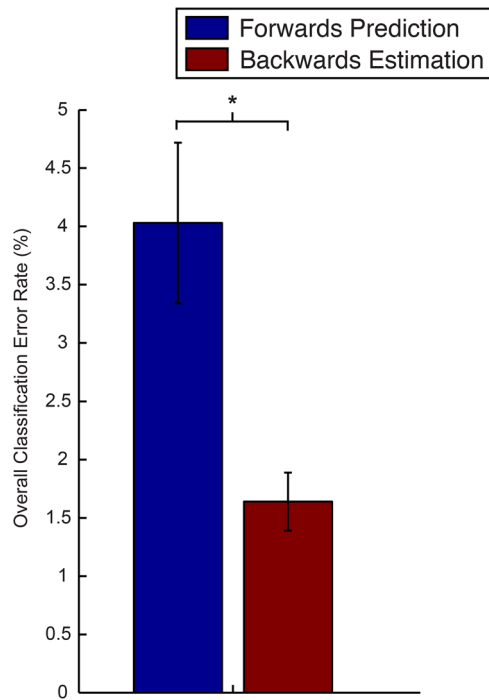


**Figure 8.** Performance of labeling strategies. The adaptive algorithm used backwards estimation to label new patterns. The figure shows the performance of the backwards estimator (red) that was used during online assessment of the adaptive algorithm compared to using the output of the online forward predictor (blue). Data are averages of eight subjects ( $\pm 1$  SEM). \* denotes statistically significant differences ( $p < 0.05$ ).

**Table 3.** Real-time computation.

Process	Average time (ms)	Standard deviation (ms)
Baseline processing	15.1	2.4
Feature extraction	2.4	0.02
Forward prediction	0.3	0.04
Backward estimation	4.6	0.2
Tracking of means, covariances	0.5	0.2
All processes	22.9	2.5

predictions in the online session increased over time. We expect that EMG data usage would increase further as users continued to ambulate with the prosthesis. In summary, the combination of the log-likelihood threshold and adaptation results in a control system that prevents errors associated with changes in EMG, but also learns from these changes to create a robust model of EMG data over time.

Comparisons between adaptive and non-adaptive algorithms showed that the adaptive system performed significantly better. A static algorithm that used only mechanical sensors would have had more errors than the adaptive algorithm used in the online sessions, suggesting that updating EMG provides a small, but statistically significant improvement in classification performance. Moreover, a static algorithm that used mechanical sensors, EMG, and a log-likelihood threshold also would have performed significantly worse than the adaptive algorithm. This indicates that using EMG signals across days, even with a log-likelihood threshold, is not optimal; updating

the model of EMG data via adaptation provides the best performance. However, our comparison of online and offline performance does not take into account the interaction between user and control system that occurs only in online systems and is critical in understanding performance. A more appropriate comparison would be an online analysis of adaptive and non-adaptive versions of the algorithm. However, the comparison between online and offline performance performed here is not uninformative. Understanding how other systems would have performed is still useful; knowledge of what forward prediction errors the non-adaptive systems would have made provides an idea of how many mistakes were prevented by EMG adaptation. Since forward prediction misclassifications can provide significant perturbations to the user that can endanger their safety, it is preferable to gain this knowledge without the risk of a stumble or a fall.

The benefit provided by adaptation of EMG observed in this study is smaller than observed in our previous experiments, which demonstrated that including EMG into forward predictions produced a decrease in online error rates from 14.1%, when only mechanical sensor data were used, to 7.9% with the addition of EMG data [4, 5]. To explain this finding, we conducted an offline analysis to investigate the effect of our control system modifications on forward predictor performance. Our analysis showed that these modifications decreased the error rate of the forward predictor, and that combining these modifications resulted in the lowest error rates. More importantly, the analysis revealed that the benefit of including EMG signals is much less apparent when these control system modifications are included. Thus, although our adaptive algorithm learned to reincorporate EMG signals into its predictions, the benefit of including EMG was marginal given the improvements already made to the control system. This finding is important because it suggests that EMG may not be necessary for locomotion mode prediction in powered lower limb devices, and that other approaches (e.g. choice of classifier architecture, mechanical sensors, or the timing of mode transitions) could provide similar benefits to EMG, which is cumbersome to implement. However, it should also be noted that EMG signals encoding user intent could be used to accomplish other important tasks beyond locomotion mode prediction, for example, volitional actuation of prosthetic joints to reposition the device or detection and prevention of falls or stumbles.

Other factors could contribute to the reduced benefit of including EMG information. First, acquiring and implementing EMG information for lower limb prosthesis control during the dynamic task of ambulation is challenging, and, as a result, acquired EMG data were likely not of the highest quality. Further efforts are needed to develop EMG acquisition systems that seamlessly integrate with lower limb prostheses and acquire high quality EMG data during ambulation. Second, it is possible that more data were required to build a representative model of EMG data; however, obtaining a large amount of data is challenging and requires long, burdensome experimental sessions. Third, the adaptive system used in this analysis simply pooled newer EMG data with prior EMG data. It is possible that the EMG data acquired from



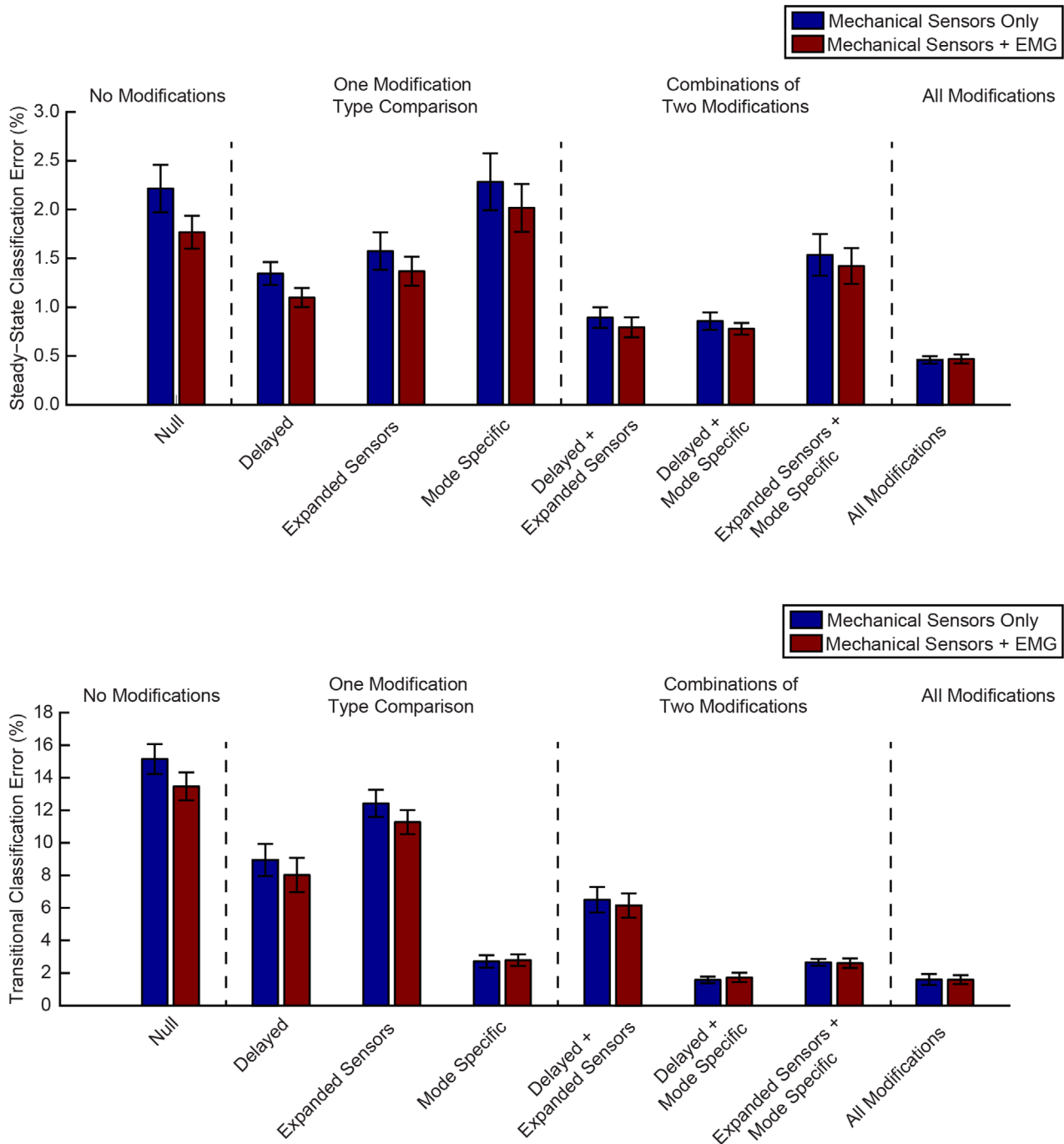


**Figure 9.** Effect of control system modification on forward prediction steady-state (top) and transitional (bottom) error rates. The effect of four different modifications to the prosthesis control system—delayed transitions, expanded mechanical sensors, and mode specific classifier architecture—on forward prediction were compared separately and in all possible combinations with each other. Two types of forward predictors were compared—one that used only mechanical sensor signals (blue bars), and one that used the combination of EMG signals and mechanical sensors (red bars). Data are averages of eight subjects, error bars represent  $\pm 1$  SEM.

a previous experimental session may interfere with tracking changes in EMG signals. While it is unclear that this actually happened in this study, this issue could be addressed by incorporating a forgetting factor. A forgetting factor would ‘forget’ or remove ‘older’ patterns as the system is building a newer model of EMG data. In this circumstance, the adaptive system would make forward predictions with only the most recent set of EMG data. Further work is needed to address these issues.

We also analyzed the types of errors the adaptive forward predictor made. We found that overall, each subject could transition between the required locomotion modes and complete the different activities using the online system with low error rates. Transitions to and from ramp descent were the most problematic for the forward predictor. Typically, these errors only presented a minor perturbation to the user. More substantial errors (e.g. inappropriately transitioning into

stair ascent mode) cause much larger perturbations and may endanger the patient, but rarely happened. It is worth noting that the descriptions of the perturbations in this study are more anecdotal rather than based on quantitative analyses of stability or change in mechanical work [25]. The user's feedback on which errors are noticeable and/or dangerous will need to be considered alongside the forward predictor's confusion matrices to fully determine what error rate is acceptable for prosthetic control.

Similar to a previous offline study [23], the backward estimation labeling strategy was able to label new patterns in real-time with a very low error rate (1.64% [0.25%]). This labeling strategy worked in an online setting where incorrect forward predictions may alter the gait patterns of the user, which could have impacted the ability of the backwards estimator to label data. However, backwards estimation is reliable because the locomotion modes are preprogrammed in the prosthesis, and ambulation is cyclical, allowing steps to be accurately classified. The main advantage of this strategy is that it is statistically more accurate at labeling patterns than the forward predictor. Backwards estimation is also able to accurately classify steps when the forward predictor makes an error (i.e. prosthesis is in the wrong mode). We pre-programmed the backward estimator to recognize when the prosthesis was in the incorrect mode (e.g. when the user was ambulating down an incline but the prosthesis was still in level-ground walking mode), thus we can correctly infer user intent despite mistakes made by the forward predictor. We expect this method to be even more useful in across-user applications, where higher forward predictor error rates may occur. It may be possible to improve the backwards estimator's performance by incorporating knowledge of the user's previous mode transitions. These prior knowledge approaches have been shown to be useful for forward prediction, where information about which modes transitions the user completed in the past [36] or which modes transitions are allowed by the state machine is very useful in making future predictions [28]. The backwards estimator in this study did not incorporate this information, and its utility should be investigated in future studies.

We took a number of steps to ensure that our adaptive algorithm (and this study as whole) was computationally and practically efficient. In practice, performing real-time ambulation experiments using powered leg prostheses are challenging and time-consuming. Often, an hour is required for the user to don the custom fabricated instrumented socket, verify that the fit is comfortable, ensure that the device is properly aligned, and verify that the EMG signals are of a reasonable quality. This setup time, along with providing adequate periods of rest for the patient between activities, limits the overall number of steps that can be collected for each type of activity. To prevent overfitting of our models, we used PCA or ULDA based on an analysis of pilot data, and took the approach that we would implement the method that allowed for the fewest representative features to be used so that the real-time performance of the adaptive algorithm could be optimized. These implementations helped ensure that our adaptive algorithm ran efficiently in real-time. All processes needed for the prosthesis to function appropriately were completed within the 30 ms frame

increment (though it should be noted that this chosen increment is somewhat arbitrary and perhaps could be decreased without any detriment to the user). In addition, our algorithm updated the classifiers of the forward predictor frequently (125 times in 10 min), allowing for fast adaptation incorporating the newest sensor data. Our online implementation is particularly important because it is critical to evaluate control algorithms in users. In our study, errors made by the online control system affected users' ambulation, making it more likely for the control system to make another error. Offline studies do not capture this human-machine interaction and resulting error propagation. Thus, an online study presents the most accurate representation of algorithm performance.

In conclusion, this study demonstrates improved control of robotic lower limb prostheses using pattern recognition systems that adapt to changes in input signals, specifically EMG signals. We demonstrated that the adaptive algorithm could learn a new model of EMG data acquired across experimental sessions, and that this adaptation prevented errors that would have been made by non-adaptive algorithms. We also determined that control system modifications implemented prior to this experiment improved classification accuracy and thus decreased the benefit provided by EMG information. However, our adaptive algorithm moves pattern recognition control systems for lower limb prostheses towards clinical viability by addressing a main limitation of myoelectric interfaces: the inability to track, and adapt to, EMG signal changes. More broadly speaking, adaptation of control signals encoding user intent allows assistive devices to respond to the user's behavior and operate in sync with the user in many different environments, across long periods of time. Thus, we expect our adaptive algorithm to be robust and useful in other applications, including across-user applications. Adaptation could also be used to update the model of mechanical sensor data and create intent recognition systems for novel users during ambulation. We have demonstrated this application in preliminary studies, and will fully investigate it in future studies.

## 5. Conclusion

In this study we developed an adaptive pattern recognition system for a robotic lower limb prosthesis that adapts to changes in the user's neural information during ambulation. The adaptive system continuously updated the user's model of neural data and accurately and consistently identified the user's intent over multiple days, despite changing neural signals. We found that our adaptive control system outperformed non-adaptive versions of the control system, and that adaptation resulted in significantly lower system error rates. The results of this study are encouraging and provide another step towards a clinically viable EMG-based intent recognition system for robotic assistive devices.

## Acknowledgments

This work was supported by the US Army's Telemedicine and Advanced Technology Research Center (TATRC) contract

WW81XWH-09-2-0020, the US Army's Joint Warfighter Program contract W81XWH-14-C-0105, the National Institute of Health NIH R01 HD079428-02, and Northwestern University's John N Nicholson grant. Author LH is an inventor on the related patent 9443203.

## ORCID iDs

J A Spanias  <https://orcid.org/0000-0001-7691-7622>

## References

- [1] Contreras-Vidal J L and Grossman R G 2013 NeuroRex: a clinical neural interface roadmap for EEG-based brain machine interfaces to a lower body robotic exoskeleton *Conf. Proc. Annu. Int. Conf. IEEE Engineering in Medicine and Biology Society* vol 2013 pp 1579–82
- [2] Lawson B E, Mitchell J E, Truex D, Shultz A, Ledoux E and Goldfarb M 2014 A robotic leg prosthesis *IEEE Robot. Autom. Mag.* **21** 70–81
- [3] Duvinage M, Castermans T, Jiménez-Fabián R, Hoellinger T, De Saedeleer C, Petieau M, Seetharaman K, Cheron G, Verlinden O and Dutoit T 2012 A five-state P300-based foot lifter orthosis: proof of concept 2012 *ISSNIP Biosignals and Biorobotics Conf.: Biosignals and Robotics for Better and Safer Living (BRC)* pp 1–6
- [4] Huang H, Zhang F, Hargrove L J, Dou Z, Rogers D R and Englehart K B 2011 Continuous locomotion-mode identification for prosthetic legs based on neuromuscular—mechanical fusion *IEEE Trans. Biomed. Eng.* **58** 2867–75
- [5] Hargrove L J, Young A J, Simon A M, Fey N P, Lipschutz R D, Finucane S B, Halsne E G, Ingraham K A and Kuiken T A 2015 Intuitive control of a powered prosthetic leg during ambulation: a randomized clinical trial *J. Am. Med. Assoc.* **313** 2244–52
- [6] Sup F, Bohara A and Goldfarb M 2008 Design and control of a powered transfemoral prosthesis *Int. J. Robot. Res.* **27** 263–73
- [7] Au S, Berniker M and Herr H 2008 Powered ankle-foot prosthesis to assist level-ground and stair-descent gaits *Neural Netw.* **21** 654–66
- [8] Bellman R D, Holgate M A and Sugar T G 2008 SPARKy 3: design of an active robotic ankle prosthesis with two actuated degrees of freedom using regenerative kinetics 2008 *2nd IEEE RAS and EMBS Int. Conf. on Biomedical Robotics and Biomechatronics* pp 511–6
- [9] Varol H A, Sup F and Goldfarb M 2008 Real-time gait mode intent recognition of a powered knee and ankle prosthesis for standing and walking 2008 *2nd IEEE RAS and EMBS Int. Conf. on Biomedical Robotics and Biomechatronics* pp 66–72
- [10] Zhang F, Fang Z, Liu M and Huang H 2011 Preliminary design of a terrain recognition system *Proc. Annual Int. Conf. IEEE Engineering in Medicine and Biology Society EMBS* pp 5452–5
- [11] Tucker M R, Olivier J, Pagel A, Bleuler H, Bouri M, Lamercy O, Millán J D R, Riener R, Vallery H and Gassert R 2015 Control strategies for active lower extremity prosthetics and orthotics: a review *J. Neuroeng. Rehabil.* **12**
- [12] Hoover C D, Fulk G D and Fite K B 2012 The design and initial experimental validation of an active myoelectric transfemoral prosthesis *J. Med. Device* **6**
- [13] Dawley J A, Fite K B and Fulk G D 2013 EMG control of a bionic knee prosthesis: exploiting muscle co-contractions for improved locomotor function 2013 *IEEE Int. Conf. on Rehabilitation Robotics (ICORR)* pp 1–6
- [14] Jin D, Yang J, Zhang R, Wang R and Zhang J 2006 Terrain identification for prosthetic knees based on electromyographic signal features *Tsinghua Sci. Technol.* **11** 74–9
- [15] Young A J, Simon A M and Hargrove L J 2014 A training method for locomotion mode prediction using powered lower limb prostheses *IEEE Trans. Neural Syst. Rehabil. Eng.* **22** 671–7
- [16] Young A, Simon A and Hargrove L 2013 An intent recognition strategy for transfemoral amputee ambulation across different locomotion modes 2013 *35th Annual Int. Conf. of the IEEE EMBS* pp 1587–90
- [17] Lawson B E, Varol H A and Goldfarb M 2011 Standing stability enhancement with an intelligent powered transfemoral prosthesis *IEEE Trans. Biomed. Eng.* **58** 2617–24
- [18] Shultz A H, Lawson B E and Goldfarb M 2015 Running with a powered knee and ankle prosthesis *IEEE Trans. Neural Syst. Rehabil. Eng.* **23** 403–12
- [19] Lawson B E, Varol H A, Huff A, Erdemir E and Goldfarb M 2013 Control of stair ascent and descent with a powered transfemoral prosthesis *IEEE Trans. Neural Syst. Rehabil. Eng.* **21** 466–73
- [20] Hargrove L, Englehart K and Hudgins B 2008 A training strategy to reduce classification degradation due to electrode displacements in pattern recognition based myoelectric control *Biomed. Signal Process. Control* **3** 175–80
- [21] Spanias J A, Perreault E J and Hargrove L J 2016 Detection of and compensation for EMG disturbances for powered lower limb prosthesis control *IEEE Trans. Neural Syst. Rehabil. Eng.* **24** 226–34
- [22] Basmajian J V 1985 Muscles alive. Their functions revealed by electromyography *J. Med. Educ.* **37** 201–2
- [23] Spanias J A, Perreault E J and Hargrove L J 2014 A strategy for labeling data for the neural adaptation of a powered lower limb prosthesis 2014 *36th Annual Int. Conf. of the IEEE Engineering in Medicine and Biology Society (EMBC)* pp 3090–3
- [24] Spanias J A, Simon A M, Ingraham K A and Hargrove L J 2015 Effect of additional mechanical sensor data on an EMG-based pattern recognition system for a powered leg prosthesis 2015 *7th Int. IEEE/EMBS Conf. on Neural Engineering (NER)* pp 22–4
- [25] Zhang F, Liu M and Huang H 2015 Effects of locomotion mode recognition errors on volitional control of powered above-knee prostheses *IEEE Trans. Neural Syst. Rehabil. Eng.* **23** 64–72
- [26] Zhang F, Liu M and Huang H 2015 Investigation of timing to switch control mode in powered knee prostheses during task transitions *PLoS One* **10** e0133965
- [27] Simon A M, Spanias J A, Ingraham K A and Hargrove L J 2016 Delaying ambulation mode transitions in a powered knee-ankle prostheses 2016 *38th Annual Int. Conf. of the IEEE Engineering in Medicine and Biology Society (EMBC)* pp 5079–82
- [28] Young A J and Hargrove L J 2016 A classification method for user-independent intent recognition for transfemoral amputees using powered lower limb prostheses *IEEE Trans. Neural Syst. Rehabil. Eng.* **24** 217–25
- [29] Hargrove L J, Simon A M, Lipschutz R, Finucane S B and Kuiken T A 2013 Non-weight-bearing neural control of a powered transfemoral prosthesis *J. Neuroeng. Rehabil.* **10** 62
- [30] Tkach D C, Young A J, Smith L H, Rouse E J and Hargrove L J 2014 Real-time and offline performance of pattern recognition myoelectric control using a generic electrode grid with targeted muscle reinnervation patients *IEEE Trans. Neural Syst. Rehabil. Eng.* **22** 727–34

- [31] Simon A M, Ingraham K A, Fey N P, Finucane S B, Lipschutz R D, Young A J and Hargrove L J 2014 Configuring a powered knee and ankle prosthesis for transfemoral amputees within five specific ambulation modes *PLoS One* **9** e99387
- [32] Simon A M, Ingraham K A, Spanias J A, Young A J and Hargrove L J 2016 Development and preliminary testing of a flexible control system for powered knee-Ankle prostheses 2016 6th IEEE RAS/EMBS Int. Conf. on Biomedical Robotics and Biomechatronics (BioRob) pp 704–9
- [33] Simon A M, Ingraham K A, Spanias J, Young A J, Finucane S B, Halsne E G and Hargrove L J 2016 Delaying ambulation mode transition decisions improves accuracy of a flexible control system for powered knee-ankle prosthesis *IEEE Trans. Neural Syst. Rehabil. Eng.* **25** 1164–71
- [34] Sup F, Varol H A, Mitchell J, Withrow T J and Goldfarb M 2009 Preliminary evaluations of a self-contained anthropomorphic transfemoral prosthesis *IEEE/ASME Trans. Mechatron.* **14** 667–76
- [35] Sup F, Varol H A and Goldfarb M 2011 Upslope walking with a powered knee and ankle prosthesis: initial results with an amputee subject *IEEE Trans. Neural Syst. Rehabil. Eng.* **19** 71–8
- [36] Young A J, Simon A M, Fey N P and Hargrove L J 2014 Intent recognition in a powered lower limb prosthesis using time history information *Ann. Biomed. Eng.* **42** 631–41
- [37] Varol H A, Sup F and Goldfarb M 2010 Multiclass real-time intent recognition of a powered lower limb prosthesis *IEEE Trans. Biomed. Eng.* **57** 542–51
- [38] Hudgins B, Parker P and Robert N 1993 A new strategy for multifunction myoelectric control *IEEE Trans. Biomed. Eng.* **40** 82–94
- [39] Huang Y, Englehart K B, Hudgins B and Chan A D C 2005 A Gaussian mixture model based classification scheme for myoelectric control of powered upper limb prostheses *IEEE Trans. Biomed. Eng.* **52** 1801–11
- [40] Jolliffe I T 2002 *Principal Component Analysis* 2nd edn (Berlin: Springer) ([https://doi.org/10.1007/0-387-22440-8\\_7](https://doi.org/10.1007/0-387-22440-8_7))
- [41] Yuan D, Liang Y, Yi L, Xu Q and Kvalheim O M 2008 Uncorrelated linear discriminant analysis (ULDA): a powerful tool for exploration of metabolomics data *Chemom. Intell. Lab. Syst.* **93** 70–9
- [42] Vidovic M, Hwang H-J, Amsuss S, Hahne J, Farina D and Ruller M K 2015 Improving the robustness of myoelectric pattern recognition for upper limb prostheses by covariate shift adaptation *IEEE Trans. Neural Syst. Rehabil. Eng.* **24** 961–70